Adsorption behavior of anionic surfactants to silica surfaces in the presence of calcium ion and polystyrene sulfonate

Liu, Zilong; Hedayati, Pegah; Sudhölter, Ernst J.R.; Haaring, Robert; Shaik, Abdur Rahman; Kumar, Naveen

DOI
10.1016/j.colsurfa.2020.125074

Publication date
2020

Document Version
Final published version

Published in
Colloids and Surfaces A: Physicochemical and Engineering Aspects

Colloids and Surfaces A 602 (2020) 125074

Contents lists available at ScienceDirect

Colloids and Surfaces A

journal homepage: www.elsevier.com/locate/colsurfa

Adsorption behavior of anionic surfactants to silica surfaces in the presence of calcium ion and polystyrene sulfonate

Zilong Liu*, Pegah Hedayati, Ernst J.R. Sudhölter*, Robert Haaring, Abdur Rahman Shaik, Naveen Kumar

Organic Materials & Interfaces, Department of Chemical Engineering, Faculty of Applied Sciences, Delft University of Technology, Van der Maasweg 9, 2629 HZ Delft, the Netherlands

GRAPHICAL ABSTRACT

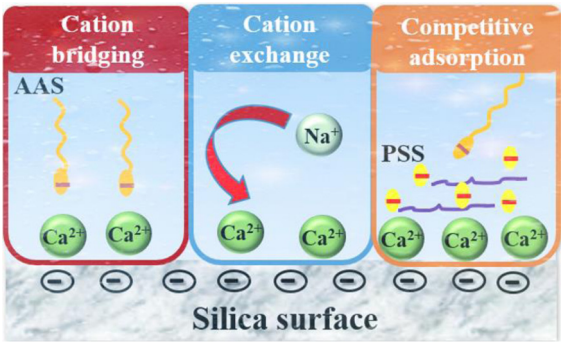

ARTICLE INFO

Keywords:
Surfactant adsorption
Salt solution
Polyelectrolyte
QCM-D
Enhanced oil recovery

ABSTRACT

Adsorption behavior of surfactants to rock surfaces is an important issue in oil recovery, especially in the process of surfactant flooding. The surfactant loss through adsorption to rock surfaces makes such process economically less feasible. Here, we investigated the adsorption behavior of anionic surfactants (alcohol alkoxy sulfate, AAS) onto silica with quartz crystal microbalance with dissipation monitoring. The results demonstrated that the surfactant adsorption followed the Langmuir adsorption isotherm. Up to solution pH 10, surfactant adsorption slightly increased with increasing pH. The higher pH leads to more anionic surface sites for binding with an anionic surfactant with the help of a calcium cation bridging. The amount of anionic surfactant binding also increases with increasing calcium ion concentration up to 50 mM. It was found that sodium ions were able to exchange calcium ions near the silica surface, which would reduce the affinity for surfactant adsorption. The effect of the polyanion polystyrene sulfonate (PSS) on the anionic AAS adsorption was investigated to learn the possible competitive adsorptions. Indeed, this was found. Upon addition of 50 ppm PSS to a 0.05 wt% AAS containing solution, the adsorption of AAS was reduced by about 85 %. The obtained results show the interplay of different interacting species affecting the overall degree of anionic surfactant adsorption to silica surfaces. Optimal tuning of the process conditions according to these results will contribute to a more efficient use of anionic surfactants in enhanced oil recovery.

* Corresponding authors.
E-mail addresses: zlliu89@gmail.com (Z. Liu), E.J.R.Sudholter@tudelft.nl (E.J.R. Sudhölter).

https://doi.org/10.1016/j.colsurfa.2020.125074
Received 9 April 2020; Received in revised form 25 May 2020; Accepted 26 May 2020
Available online 31 May 2020

1. Introduction

With the increase of oil production demand, surfactant flooding as part of enhanced oil recovery (EOR) is receiving substantial attention [1–3], and has been used to trigger residual oil release and to acquire higher recoveries from reservoir rocks. The injected batches of surfactant solutions contribute to the reduction of the oil-water interfacial tension, to alter the wettability, and for foam generation [4–8]. The main problem that often makes the surfactant flooding process inefficient and economically less feasible is surfactant losses because of their adsorption to the reservoir rocks [9,10]. Among various surfactant based EOR methods, a low adsorption is a significant requirement to achieve effective transportation of surfactants into the mineral matrixes. To minimize surfactant adsorption, it is necessary to well understand the adsorption behavior of surfactants.

In surfactant-water-rock systems, the adsorption process of surfactants mainly contains four steps [11–13]. The first step is surfactant adsorption through electrostatic interactions between hydrophilic head groups of surfactants and the charged sites of rock surfaces. The second step involves the interaction of hydrophobic parts of ongoing surfactants in solution with previously adsorbed surfactants, leading to surface aggregates such as hemi-micelles. In the third step adsorption takes place because of hydrophobic interactions with a reduced rate. Above the critical micelle concentration (CMC), the surfactant monomer concentration is more or less constant, and any increase of surfactant concentration only contributes to more micelles, which does no change the maximum adsorption in the final step [13]. The amount of surfactant adsorption relies on the chemistry of the rock (*i.e.*, its chemical compositions and surface charges), the kinds of surfactants, and water chemistry (*i.e.*, salinity, present ions, solution pH) [6,7,13–16]. Several research covering various aspects of the adsorption process have been studied, including the adsorption kinetic behavior [8], adsorption isotherm [14], adsorption mechanism [13], and the structure of the adsorbed surfactant layer [11,17,18]. So far, no systematic study has appeared to explore the effect of various cations and polyelectrolytes on the surfactant adsorption.

The charge of a mineral surface can be positive or negative by the dissociation behavior of the mineral constituents or by the adsorption of ions from the aqueous medium. It is well known that near neutral pH silica surfaces are negatively charged, while carbonate surfaces are positively charged surfaces [1,19]. Cationic surfactants prefer to adsorb on negatively charged surfaces, and anionic surfactants are attracted to positively charged surfaces. Adjustments of the solution pH can influence the surface charge, and thereby alter the amount of adsorbed surfactants. It was revealed that the adsorption of anionic surfactants to silica surfaces was largely reduced, when solution pH went up to 11 [20]. Often, anionic surfactants are used widely in sandstone reservoirs due to the fact of less adsorption in comparison to nonionic, cationic and zwitter-ionic surfactants [21]. The adsorption behavior of sodium dodecyl benzene sulfonate onto kaolinite showed that it was better fitted with the Langmuir model than the Freundlich model [14]. This result was consistent with Achinta et al. [22], who pointed out that the Langmuir isotherm suited the equilibrium adsorption of surfactants to the sandstone surface.

The ionic composition of the injected solution has been found to play an important part in the surfactant adsorption to the rock surfaces and therefore contributed to their losses in the reservoirs [23–25]. The divalent cations like Ca^{2+} can result in a substantial increase of anionic surfactants adsorption to negatively charged surfaces; on the other hand, their presence does decrease the amount of cationic surfactant adsorption [7,25,26]. On silica surfaces the amount of adsorbed sodium dodecyl sulfate doubles if the present sodium ions are replaced by calcium ions [27]. This implies that divalent cations have a stronger charge screening than monovalent cations. In addition, the divalent cations are able to form a bridge between the anionic surfactant and the negatively charged surface, favoring the adsorption. The anionic surfactants adsorption generally increased with the salinity and divalent cation concentration in solutions [28,29].

In order to reduce anionic surfactant adsorption to the reservoir rocks, alkali (sodium carbonate) has been used as a sacrificial agent [4]. The addition of alkali was not only to increase the solution pH, but also to make a more negatively charged surface, which resulted in a significant decrease of anionic surfactant adsorption to the mineral surfaces owing to electrostatic repulsions [28]. In mixtures of anionic polyelectrolytes and anionic surfactants, the overall adsorption is a competitive process. If adsorption of a polyelectrolyte (a sacrificial agent) is favored, a relatively low adsorption of surfactants is expected. Under certain conditions, sodium polyacrylate adsorbed strongly and therefore inhibited the adsorption of anionic surfactants [30]. Lignosulfonate polymers have been applied in the surfactant flooding as a cost-effective preflush chemical to lower the surfactant loss by adsorption to rock surfaces [31]. Addition of another anionic polyelectrolyte, polystyrene sulfonate (PSS), was found to prevent adsorption of anionic surfactants from highly saline brine solutions [29,32]. Henceforth, to mitigate surfactant adsorption is a challenging task and it is important to understand surfactant adsorption behavior in the presence of sacrificial agents.

Considering the above-mentioned issues, the dynamic adsorption behavior of an anionic alcohol alkoxy sulfate (AAS) surfactant to a silica surface was investigated at varying pH, calcium ion, sodium ion, AAS and PSS concentrations using a Quartz Crystal Microbalance with Dissipation monitoring (QCM-D). This fundamental study provides a relatively rapid methodology of investigating a range of important parameters for surfactant adsorption to rock surfaces, compared to traditional liquid chromatography [6,29], calorimetric methods [30], and core flooding measurements [33]. The purpose of this work is (i) to systematically explore the processes that dominate the adsorption behavior of AAS surfactant with varying pH, salt concentrations, and mixed solutions containing both calcium and sodium ions, (ii) to obtain an improved understanding of the adsorption mechanism of AAS surfactant and PSS polyelectrolyte, and (iii) to gain insights into the influence of PSS on the adsorption behavior of AAS, which contributes to reduce surfactant losses in EOR by adsorption.

2. Experimental methods

2.1. Materials and solutions

The anionic AAS surfactant with a molecular weight (MW) of 700 g/mol was provided by Shell Global Solutions. This surfactant contained mainly C_{12}/C_{13} alkyl tails and 7 propoxy units in the middle associated with a sulfate head group. Such a surfactant is commonly used in EOR, which had an excellent divalent cation tolerance without precipitations in a higher concentrations and was cheaper in comparison to other EOR surfactants [34]. Poly(sodium 4-styrenesulfonate) (PSS, MW = 70,000 g/mol) is an anionic polyelectrolyte and was purchased from Sigma-Aldrich. Each PSS chain has ~340 monomeric units carrying an anionic sulfonate group. The molecular structures of AAS and PSS are displayed in Fig. 1a, and the compounds were used as collected without any treatment. The salt solutions were made by mixing the reagent-grade salts (NaCl, $MgCl_2$, and $CaCl_2$, with purity grades of > 97.0 % from Sigma-Aldrich) with ultrapure deionized water (resistivity of > 18.2 MΩ cm, Milli-Q). The surfactant solution was prepared by adding a certain amount of surfactants into prepared salt solutions, then was shaken using a vortex shaker (Scientific Industries, Vortex-Genie 2) for 30 min at intensity 5. After that, well dispersed and stable solutions were obtained. A Metrohm 827 pH meter was used to monitor the solution pH, which was regulated by using drops of 0.2 M HCl and 0.2 M NaOH.

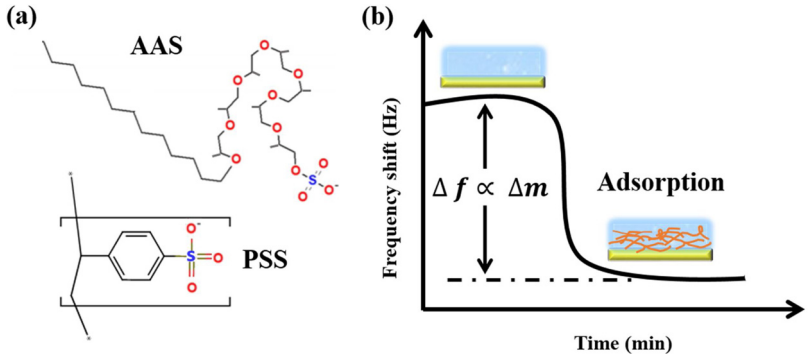

Fig. 1. (a) The molecular structures of AAS surfactant and PSS polyelectrolyte. (b) Schematic diagram of a typical adsorption experiment, where the frequency shift is monotonically related to the mass adsorbed to the silica coated sensor surface.

2.2. Silica sensors

The silica (QSX 303, Q-sense) standard coated sensors were purchased from Biolin Scientific. Typically silica is considered as representative of sandstone rocks, and these rocks contains impurities of clay and alumina. We have investigated surfactant adsorption on clay minerals [10], therefore, this study focused on the silica surfaces and a more complex surface can be in the further research. The silica sensor has an AT-cut quartz crystal disk with a diameter of 14 mm and the fundamental resonance frequency (f_0) of the silica crystal is 5 MHz. To eliminate any surface contaminations, the silica sensors were rinsed sequentially with Milli-Q water, ethanol, and *iso*-propanol, overall three times prior to each measurement. Successively, it was mildly dried in a stream of clean nitrogen gas. Then, the dried sensor was air plasma cleaned at 1000 mTorr (Harrick Plasma Cleaner, 110 V) with a moderate intensity for 5 min. Finally, the clean sensor was instantly put into the flow modules at the desired position. The sensors can be reused for a few times that depended on the reproducibility of signals in the measurement. To reduce signal drifts, each sensor was used no more than five times.

2.3. Surface characterizations and surface tensions

The silica surface was scanned in tapping mode using Atomic Force Microscopy (AFM, NT-MDT), with a silicon tip (NSG03, NT-MDT) that had a nominal radius of 7 nm and a nominal spring constant of 0.4–2.7 N/m. Topography images were obtained over a 5 × 5 μm^2 area with 512 × 512 data points, at a scan rate of 1 Hz. As shown in Fig. S1, the silica surface is very smooth, with a root mean square height of 1.5 nm. We used the Wilhelmy plate method to measure the relation between surface tension and AAS surfactant monomer concentration. A thin platinum plate was cleaned thoroughly in a gas burner flame. The variation of surface tension for an aqueous AAS surfactant solution as a function of the surfactant concentration on a logarithmic scale is given in Fig. S2. The CMC of AAS is ~0.005 wt% (0.07 mM) in 50 mM $CaCl_2$ and pH 9.5.

2.4. QCM-D principles

Quartz Crystal Microbalance with Dissipation monitoring (QCM-D) has been applied broadly in the study of the adsorption behavior of organic molecules onto rock surfaces with the nanogram sensitivity [19,25]. A QCM-D (E1, Q-sense) was used to explore the adsorption behavior of AAS surfactant to silica surfaces. It can simultaneously monitor the changes of the resonant frequency and dissipation of the silica sensors. When an alternating voltage is implemented to the electrodes, the shear stress is produced, which induces an oscillation of the silica crystal at its fundamental resonance frequency (f_o). The increased mass (Δm) bound to the crystal surface would result in a negative frequency shift (Δf). The Sauerbrey equation showed a linear relationship between Δf and Δm, expressed as [35]:

$$\Delta f = -\frac{2nf_0^2\Delta m}{\rho_q v_q} = -\frac{n\Delta m}{C} \quad (1)$$

where n is the overtone number (1, 3, 5, etc.), C is the sensitivity constant of the quartz crystal sensor (equals 0.177 mg m^{-2} Hz^{-1}), ρ_q is the specific density (2650 kg/m^3), and v_q is the shear wave velocity (3340 m/s). When the adsorbed material is thin, rigid, uniformly distributed, and does not slip at the rock-water interface, the Sauerbrey equation is valid [36]. This may well be the case for small surfactant molecules, but can be violated by higher MW polymers. The Newtonian fluids flow through the oscillating crystal, the frequency shift due to the viscosity and density effect of the solution (liquid loading) was estimated as follows [37].

$$\Delta f_{liquid\ loading} = -\sqrt{\frac{n}{\pi}}\frac{2f_0^{1.5}}{\rho_q v_q}(\sqrt{\rho_1\mu_1} - \sqrt{\rho_2\mu_2}) \quad (2)$$

where subscripts 1 and 2 refer to the solution of diff ;erent viscosities and densities, respectively. The viscosity and density of salt solutions were assumed similar to the salt solutions with only a tiny amount of surfactant addition (~0.15 wt%, 2.1 mM). Therefore, the liquid loading effect assumed to be the same for salt and surfactant solutions. In this picture, the amount of adsorbed surfactants was calculated from the frequency difference between salt and surfactant solutions, i.e., $\Delta f_{ads}(surfactants) = \Delta f_{surfactant+salts} - \Delta f_{salts}$, as shown in Fig. 1b. The average values of the QCM-D data were taken and presented for the calculations in the present study.

2.5. QCM-D experimental procedures

Before each experiment, the flow modules and connecting tubes of QCM-D also need cleaning, by following the same process as used for rinsing the silica sensor but without a plasma treatment. At a constant flow rate of 200 μL/min, Milli-Q water was firstly injected into the flow modules using a peristaltic pump (ISMATEC, ISM935C). At the same time, the QCM-D recorded the resonant frequency and dissipation of different overtones of crystals. It was found that the fifth harmonic of the fundamental resonance frequency revealed a better signal-to-noise ratio, which was therefore chosen for our measurements. When a stable and repeatable reference signal was obtained, the silica sensor surface was subsequently contacted with a salt solution, followed by continuing injection of the surfactant solution. The solution composition was returned to Milli-Q or salt solutions to remove the previously adsorbed surfactants. The measurements were repeated 2–4 times for each solution to guarantee the accuracy and reliability of the obtained data. At the end of each experiment, Milli-Q water was flushed with a constant flow rate of 200 μL/min during 45 min to rinse the entire system.

2.6. Adsorption isotherms

The adsorption isotherms describe the surfactant losses due to adsorption to the rock surfaces. It can be achieved by plotting the amount of adsorbed surfactant as a function of the equilibrium surfactant concentration at a specific temperature [12,14,22]. The two most common adsorption models used are the Langmuir and Freundlich models. The Langmuir type isotherm is expressed as follows:

$$\Gamma = \frac{\Gamma_{max} K_L C}{1 + K_L C} \tag{3}$$

where K_L, C, Γ, and Γ_{max} are the Langmuir equilibrium constant, the equilibrium surfactant concentration, the adsorbed amount, and the maximum amount of surfactant adsorption, respectively. The validity of the Langmuir isotherm depends on the assumption that monolayer adsorption occurs on a homogeneous surface, with no interactions among adsorbing/desorbing surfactants [13]. The Langmuir equation can be arranged into a linearized form:

$$\frac{1}{\Gamma} = \frac{1}{\Gamma_{max}} + \frac{1}{C} \bullet \frac{1}{\Gamma_{max} K_L} \tag{4}$$

From the plot, it is easy to calculate the K_L and Γ_{max} from the slope and intercept. Another important term of the Langmuir model that represents the compatibility of adsorption is the non-dimensional constant R_L, which is expressed as $R_L = 1/(1 + K_L C_0)$. Here, C_0 is the initial adsorbate concentration in the aqueous solution. The lower R_L value reflects that adsorption is more favorable. The R_L is always smaller than or equal to unity then the equilibrium lies at the adsorbed species and thus the adsorption is favorable [12,38,39].

The Freundlich model describes that the adsorption Γ is proportional to the solute concentration C to the power $1/n$, where n is a heterogeneity factor:

$$\Gamma = K_F C^{1/n} \tag{5}$$

where K_F is the Freundlich constant. It is assumed in the Freundlich model that the surface is inhomogeneous with diverse types of adsorption sites. This model does not require the adsorption to be a monolayer but also enables multilayers [14]. By taking the logarithm of Γ and plotted versus log(C), the slope of the straight line equals $1/n$ and the intercept equals to log(K_F). The value of $1/n$ is always less than or equal to 1, indicating adsorption intensity of the system. When $0.1 < 1/n < 0.5$, adsorption is thermodynamically favorable; for $0.5 < 1/n \leq 1$, adsorption is still possible [22,40]. In the present study, the adsorption behavior of surfactants and polyelectrolytes are analyzed using these two models, to find which model offers the best correlation with our experimental data. The QCM-D is also an interesting technique compared to traditional static measurements for adsorption isotherms.

3. Results and discussions

3.1. Adsorption isotherms of AAS

It is of importance to determine the amount of AAS surfactant adsorption to silica surfaces to understand this route of surfactant loss. Under the solution conditions of 50 mM $CaCl_2$, pH = 9.5 and ambient temperature, the frequency shift of the QCM-D was monitored as a function of varying AAS concentrations (Fig. 2a). The results are plotted as the maximum amount of AAS adsorption (in frequency shift numbers) as function of AAS concentration (Fig. 2b). With increasing AAS concentration, a bigger frequency shift was observed, which was explained by an increased AAS adsorption. The amount of AAS adsorbed arrives at saturation around ~0.05 wt% (= 0.7 mM), which is about ten times above the CMC ~0.005 wt% (= 0.07 mM). That the AAS adsorption to the silica surface under these conditions does not stop at arriving the CMC suggests that the affinity of AAS monomers to adsorb to the surface is similar (slightly higher) to the affinity towards the micelles. The most probable reason for the increasing adsorption above the CMC is the presence of various species in the used surfactant of technical quality. Adsorption stops as the surface is occupied. The equilibrium time is fast and around 1 min. From the observed maximal frequency shift of 30 Hz, it can be easily calculated that the mass increase equals 5.3 mg/m^2, by using the sensitivity constant of 0.177 mg/m^2 • Hz. Using the MW (AAS) =700 g/mol, this mass increase corresponds to 7.6 × 10^{-6} mol/m^2 = 4.6 molecules/nm^2. Using a cross-sectional area of 0.3 nm^2 per AAS molecule, shows that on 1 nm^2 area maximal 3 AAS molecules will fit. Experimentally we have found a number of 4.6 molecules/nm^2. This brings us to the conclusion that it is very likely that in our case a bilayer of AAS molecules has formed at the fully occupied silica surface.

The adsorption data could be very well interpreted by the Langmuir model using eq. 3, as is shown in Fig. 2b, from which are deduced Γ_{max} = -30.2 ± 1.3 Hz and K_L = 100 ± 21 L/mol • Hz. The regression coefficient (R^2) was found to be greater than 0.96, indicating good correlation with the Langmuir equation. The calculated R_L value for an initial surfactant concentration of 0.05 and 0.1 wt% were estimated to be 0.17 and 0.09, respectively, which indicates that adsorption was not very strong, but still thermodynamically favorable. This finding is in line with our interpretation that above CMC AAS adsorption to the silica surface continues (*vide supra*). There was a kink at a concentration of 0.1 wt %, which was typical for collective effects in adsorption when there were attractions between the adsorbed molecules. In such systems, at a given surface coverage, the adsorbed molecules attract additional molecules and surface phase transition could occur, leading in a step-wise jump to condensed adsorption layers. Another explanation is related to the hydrophobic interactions between the hydrophobic tails of the first surfactant adsorption layer and ongoing surfactants to form the second adsorption layer. This is not compatible with the Langmuir adsorption isotherm which assumes negligible interaction between the adsorbed molecules, but actually shows a good fitting to the experimental results. Because the mutual compensation of several factors affect the shape of the Langmuir adsorption isotherm, such as adsorption of micellizations, different surface potentials, heterogeneity of rock surfaces, lateral interaction of surfactants. It is also found that the adsorption isotherms for Ca^{2+} and Mg^{2+} resemble in Fig. S3 because they may have similar cation bridging ability for surfactant adsorption.

3.2. Effect of pH on the AAS adsorption

We have investigated the adsorption of AAS, applied at a fixed concentration of 0.15 wt% (= 2.1 mM, which is above its CMC of 0.005 wt% = 0.07 mM) to silica surfaces in the presence of 50 mM $CaCl_2$ at successively pH = 9.5, 8, 7, 6, 10 and 11. The chosen AAS concentration is often applied in EOR using this surfactant, and a pH = 9.5 resembles practical conditions. By reducing the pH, *i.e.* reducing the alkalinity of the solution, we were interested to see any effect on AAS adsorption. Increasing the pH at a later stage to 10 and 11 was to see if there is any reversibility in the adsorption behavior. In all cases 50 mM $CaCl_2$ was present. That is needed because calcium ions serve as bridges between the negatively charged silica surfaces and the negatively charged sulfate group of AAS. The results obtained are shown in Fig. 3a. Indeed, we observed, as described before, at pH = 9.5 a fast mass increase (adsorption) upon addition of 0.15 wt% AAS, and upon subsequent flushing in the absence of AAS, a slower mass decrease (desorption). Decreasing the pH to 8, 7 and 6 successively, showed a small decrease in the amount of AAS adsorption. Since the injected AAS concentration was always well above the CMC, effects of changes of AAS monomer concentration was excluded. Since the $CaCl_2$ concentration was also kept constant, this indicated that the reduced amount of AAS adsorbed was likely because of the lower negative silica surface charge density at lower pH. This assumption was consistent

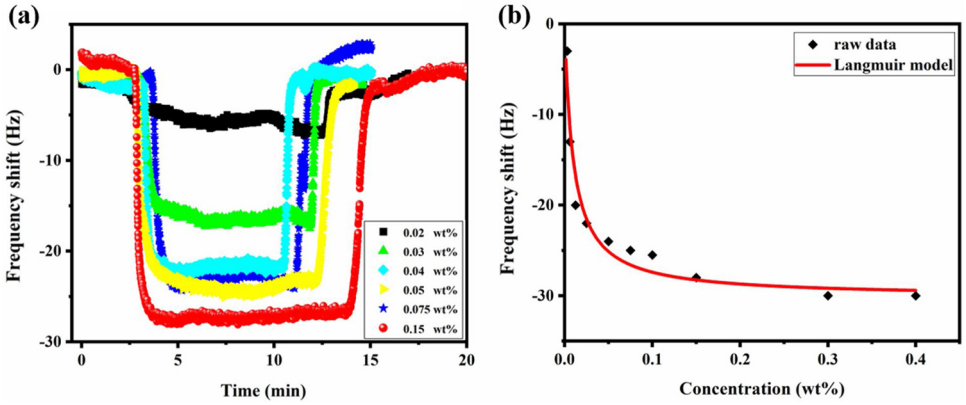

Fig. 2. (a) Real-time observed frequency shifts for the dynamic adsorption of AAS with varying concentrations, at 50 mM $CaCl_2$, pH 9.5 and ambient temperature. Parts of adsorption data were shown with some AAS concentrations. (b) The obtained data were plotted and fitted to the Langmuir adsorption model.

with previous observations [22,41–43]. Next, the applied AAS solution was set to a pH = 10, and the total amount of AAS adsorbed was slightly above the amount observed before at pH = 9.5. Further increase to pH = 11 did not increase the amount of adsorbed AAS. We have to realize here that at such a pH value the silica itself might go into solution. However, in the time framework of our experiments (20 − 30 min) we have not observed this. It is well possible that the formed AAS bilayer on the silica surface might hinder such an dissolution process. Overall, we have observed that the amount of adsorbed AAS to the silica surface responds reversibly to the external pH of the solution.

For all investigated solutions we have determined the rate of mass increase (adsorption) and mass decrease (desorption) as the time needed to from 10 to 90 % of complete adsorption and *vice versa*. Desorption was initiated by removing the AAS from the flushing solution. All other conditions were kept constant. The determined rates were obtained from the real time frequency shift data (Fig. 3a) and plotted as a function of pH (Fig. 3b). Adsorption was found always a much faster process (typically 21 ± 12 s) than desorption (typically 241 ± 33 s), showing the overall preferential binding of AAS to the silica surface. Increasing the pH showed a trend of a faster desorption, which became faster above pH > 9.5. This faster process might point to some dissolution of the silica in the high alkaline solution. Such a possible dissolution of the silica could not concluded from the earlier describes mass increase at these pH values (*vide supra*). Looking into more detail to the desorption process (Fig. S4), we observed first a fast mass decrease followed by a slower and more gradual decrease towards the final baseline. In the fast process about 30 % of the adsorbed mass was desorbed. The fast process was attributed to the desorption of the more weakly bound AAS surfactant molecules at the interface with the solution, while the slow process was most likely attributed to the desorption of the AAS surfactant molecules connected via calcium ion bridge to the silica surface. In the absence of Ca^{2+}, slight surfactant adsorption was observed with varying pH (Fig. S5). This confirmed that the presence of Ca^{2+} promoted AAS adsorption, and that at higher pH even more AAS is adsorbed, *i.e.* the more negative charged silica surfaces offers more sites for Ca^{2+} bridging.

3.3. Varying the calcium ion concentration

We have investigated the AAS adsorption to the silica modified QCM-D sensor at pH = 9.5 and ambient temperature with variable amounts of $CaCl_2$ in the range of 0.5 − 100 mM. The amount of AAS was fixed at 0.15 wt % (2.1 mM), which is well above the CMC of ~0.005 wt% (0.07 mM). We want to investigate here in which calcium ion concentration range the adsorption of AAS is affected. The results are given in Fig. 4. In the absence of calcium ions the AAS adsorption is very minor (about 2 Hz shift). Already the addition of small amounts of calcium ions induces a large frequency shift. A frequency shift of 15 Hz, i.e. half of saturation, was observed in the presence of 4 mM calcium ions. Further increase of the calcium ion concentration presents a further increase in frequency shifts (adsorbed mass increase). Above calcium ion concentrations of 50 mM, hardly any further shift is observed.

In Section 3.1 we have shown that a frequency shift of 30 Hz is most likely attributed to a bilayer of AAS surfactants adsorbed to the silica surface. It is now reasoned that a shift of 15 Hz can be attributed to a monolayer of AAS surfactants bound via calcium ion bridging to the silica surface. Thus already at very low calcium ion concentration of 4 mM, such a coverage occurs. In such a monolayer covered silica surface

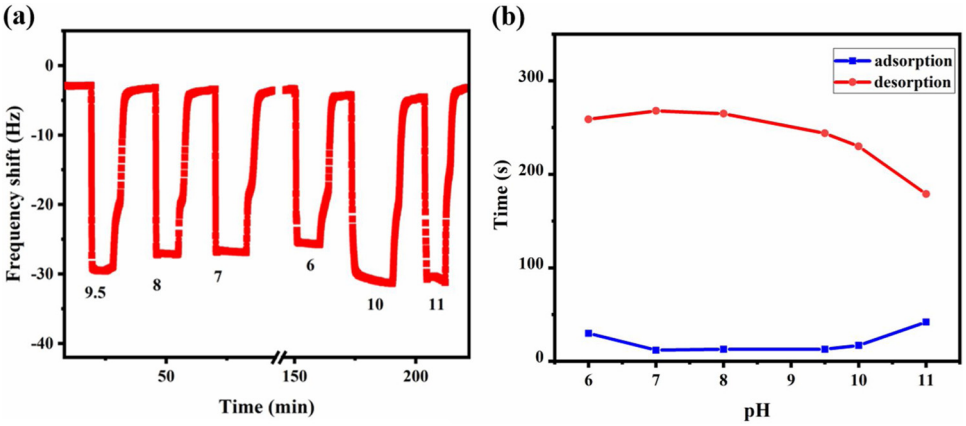

Fig. 3. (a) Real-time experimental data of frequency shifts for the AAS surfactant adsorption in 50 mM $CaCl_2$ solution, at varying pH from 6 to 11. (b) The time for complete adsorption and desorption from 10 to 90 % of AAS surfactant at different solution pH.

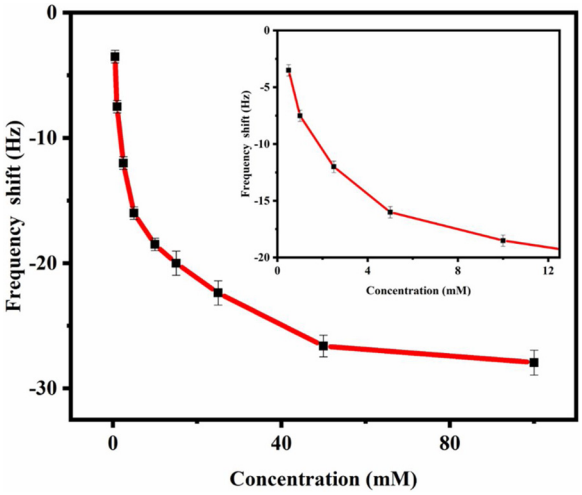

Fig. 4. Observed frequency shifts as a function of varying $CaCl_2$ concentrations (0.5-100 mM) with 0.15 wt% AAS, at pH 9.5 and ambient temperature. The inset is the magnification at the concentration range of 0-12 mM.

the surfactant hydrocarbon tails point towards the aqueous solution. This gives rise to an energetically unfavorable hydrocarbon-water interaction, which can be overcome by the formation of a bilayer. In the second layer, the hydrocarbon tails point to each other and the sulfate head group of the second layer points towards the aqueous solution. A possible intermediate state of bilayer ribbons or disks could be formed before the complete bilayer formation in which surface aggregates. The presence of a further increasing amount of calcium ions (> 4 mM) will contribute to a reduction of electrostatic repulsions between these sulfate head groups, and therefore to a stabilization of the final bilayer structure. The formation of the bilayer is how we like to interpret the frequency shift from 15 to 30 Hz upon increasing the calcium ion concentration from 4 mM to 50 mM. To obtain a detailed investigation of structural evolution, a future research with atomic force microscopy could be helpful by measuring the adsorbed layer thickness [44,45].

3.4. Mixed solutions containing both calcium and sodium ions

We have now investigated the effect of mixed NaCl and $CaCl_2$ solutions, on the AAS adsorption to silica surfaces, to see if there is any competing effect between these two ions. Firstly, we have investigated solutions containing a fixed amount of $CaCl_2 = 50$ mM and varied the NaCl between $1-500$ mM, to see any replacement of calcium ions by sodium ions. The observed real time frequency shifts are shown in Fig. 5a and the observed maximal shifts are plotted against the concentration ratio of $[Na^+]/[Ca^{2+}]$ in Fig. 5b. For low NaCl concentrations, up to 10 mM, there was a slight change observed in the frequency shift. At 50 mM of NaCl the frequency shift was reduced by *ca* 30 %, indicating that less AAS was adsorbed, and this effect became more pronounced at 100 mM of NaCl. Here, the reduction was *ca* 50 %. Thus 100 mM of NaCl in the presence of 50 mM $CaCl_2$ was able to replace about half of the surface bound calcium ions, as deduced from the 50 % reduction of AAS binding. For 500 mM of NaCl no frequency shift was observed, and therefore all the calcium ions near the surface was exchanged by sodium ions, thus AAS adsorption is no longer possible.

The process of AAS adsorption is fast with the presence of 50 mM $CaCl_2$ and NaCl concentrations below 10 mM, and the corresponding process of desorption is slow. This is in contrast to what is observed at higher NaCl concentrations. Adsorption becomes now a slow process, and desorption is a relatively faster process (Fig. 5a). This clearly indicates the reduced affinity for AAS binding in high NaCl solutions as a consequence of the displacement of the calcium ions by sodium ions. It can also be reasoned that at higher overall salt concentrations, the electrical double layer at the silica interface is more screened, leading to less electrostatic repulsions, and therefore more binding. Since in the overall process binding is reduced, it is concluded that screening is of minor importance in this situation. The observed effect that sodium ions are able to exchange calcium ions near the silica surface (as reflected by the reduced AAS adsorption) is different from our earlier results on calcite surfaces [25]. In that situation with the presence of 50 mM $CaCl_2$ and increasing NaCl concentration from 1 to 500 mM, no change in adsorption was observed. It is concluded that for calcite the surface calcium ions are much stronger bound compared to the silica calcium binding, and therefore sodium ions are not able to replace the calcium ions from the surface.

Secondly, we have kept the NaCl concentration fixed at 100 mM and varied the $CaCl_2$ concentration between $1-500$ mM, to compare with the results in the absence of NaCl (Fig. 3). The observed frequency shifts are shown in Fig. S6. It could be found that a higher $CaCl_2$ concentration is now needed to induce AAS adsorption. NaCl has a positive effect on the reduction of AAS binding in the presence of calcium ions. It was also interesting to observe the mirrored effect of Ca^{2+} to Na^+ concentration, which showed the different role of the mono- and divalent ions and their contrasting effect on the adsorption behavior. Although Na^+ is an indifferent ion without the capability of ion bridging [46], the role of calcium ions is reduced at higher salt (NaCl) concentrations,

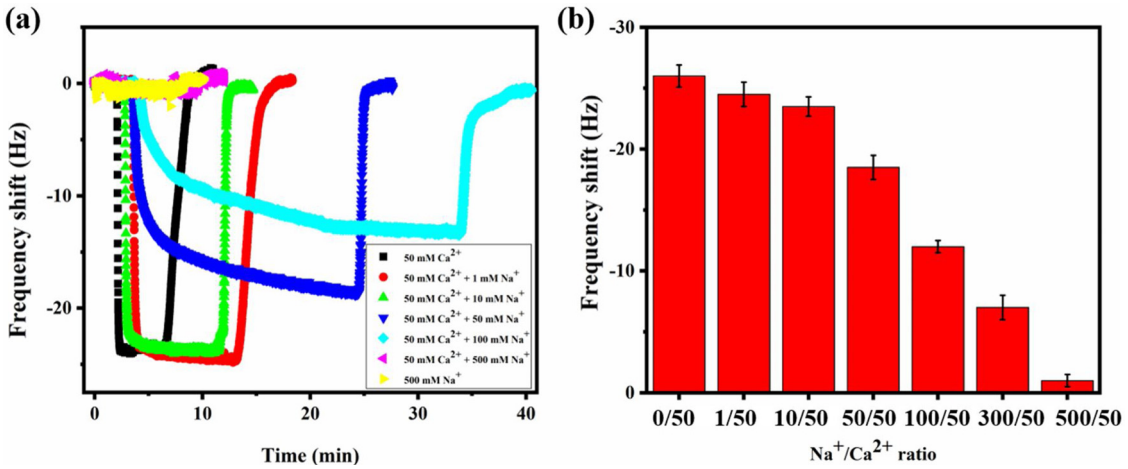

Fig. 5. (a) Real-time observed frequency shift of the QCM-D resonator upon AAS surfactant adsorption (0.15 wt%) to the silica surface with variable NaCl concentrations and a constant $CaCl_2$ concentration of 50 mM at pH = 9.5 and ambient temperature. (b) The observed maximal shifts are plotted against the concentration ratio of $[Na^+]/[Ca^{2+}]$.

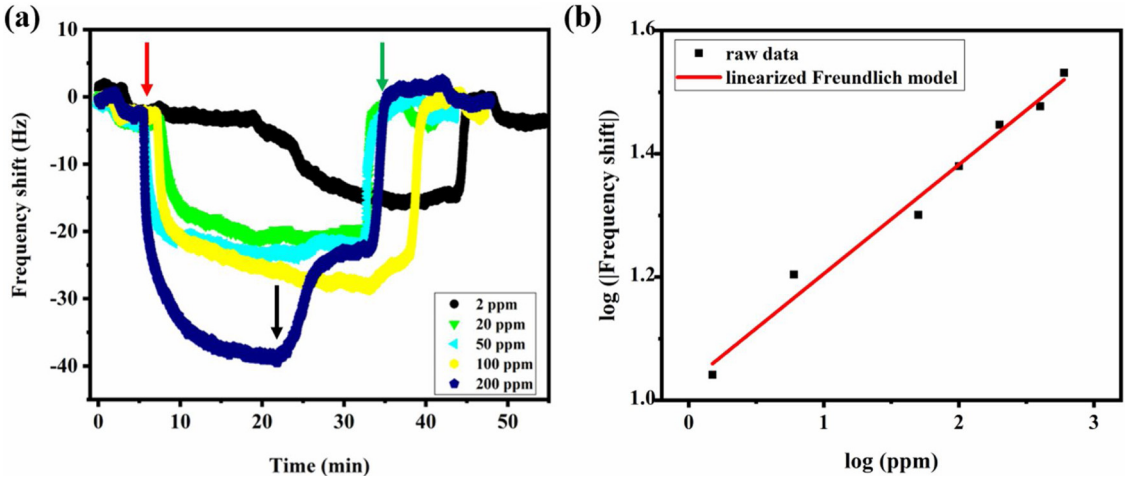

Fig. 6. (a) Real-time observed frequency shifts for the dynamic adsorption of PSS with varying concentrations, in the presence of 50 mM $CaCl_2$, at pH 9.5 and ambient temperature. Parts of adsorption data were shown with some PSS concentrations. (b) The obtained data were plotted and fitted to the linearized Freundlich model. Arrows imply the times of addition of the corresponding PSS solution (red), the injection of salt solution (black), and the full removal of surfactant by flushing Milli-Q (green) (For interpretation of the references to colour in this figure legend, the reader is referred to the web version of this article).

at least for silica surfaces. Decrease in the divalent cations and the increase of Na^+ are beneficial to the less surfactant adsorption and the concentration ratio of $[Ca^{2+}]/[Na^+]$ is also worth taking into account.

3.5. The effect of PSS addition on the AAS adsorption

Before we investigated the effect of poly(sodium 4-styrenesulfonate) (PSS) on the adsorption of AAS to silica surfaces, we have studied the PSS adsorption in the absence of AAS. Under the conditions of pH = 9.5 and 50 mM $CaCl_2$ and room temperature we have investigated the frequency shifts upon increasing the PSS concentration from 2 to 200 ppm (Fig. 6). Under these conditions we have not observed any precipitation, indicating that the solution is stable. In the absence of $CaCl_2$, no PSS adsorption was seen. In the presence of $CaCl_2$ adsorption starts already at very low PSS concentrations (2 ppm), indicating a high affinity towards surface binding. The adsorption is a relative slow process compared to the adsorption rate observed for AAS. This reflects the higher molar mass of the PSS and its concomitant slower diffusion to the surface. Increasing the PSS concentration shows an increase of adsorbed amount. The adsorption isotherm could not be fitted to the Langmuir model. This indicates that the adsorption of PSS to the surface is dependent on what is already adsorbed. This is different to our observation for the AAS adsorption. The PSS adsorption could be fitted to the Freundlich model with an excellent linear fit of $R^2 > 0.98$ (Fig. 6b), which in a good agreement with a previous study [47]. From the slope the value of $1/n = 0.18 \pm 0.01$ and the Freundlich constant of $K_F = 10.7 \pm 1$ were obtained, indicating adsorption is thermodynamically favorable. The adsorption is reversible and the desorption shows to be a two-step process. Flushing with a solution of pH = 9.5 and 50 mM $CaCl_2$ and without PSS showed that the adsorbed amount decreased in part and depended on the total amount adsorbed (Fig. 6a). Complete desorption was achieved by flushing with Milli-Q water because there will be no calcium cation bridging for the binding of PSS.

We come now to the results of our measurements in which we have investigated the effect of PSS on the AAS adsorption. All experiments were still done at 50 mM $CaCl_2$, pH = 9.5 and at ambient temperature. We have applied a solution containing 0.05 wt% AAS and 50 ppm PSS and compared the results with separate measurements on both 0.05 wt % AAS and 50 ppm PSS (Fig. 7a). From the separate experiments it is again clearly seen the fast adsorption and complete desorption of AAS by flushing with a solution of pH = 9.5 and containing 50 mM $CaCl_2$, while for the PSS situation adsorption is slow and desorption incomplete. Only flushing with Milli-Q water gives complete desorption. With this in mind, we can interpret the results obtained in the mixed experiment. Adsorption is clearly dominated by the PSS. The desorption observed in the mixed experiment shows that flushing with a solution of pH = 9.5 and 50 mM $CaCl_2$ the remaining amount of adsorbed mass is lower compared to the amount remained for the separate PSS experiment. We interpret this difference as the amount of adsorbed AAS in this situation. This amount is less compared to the amount of AAS adsorbed in the absence of PSS. The difference of less adsorbed AAS in the mixed experiment is the result of the presence of PSS. From the different frequency shifts we have estimated that about 85 % of AAS is less adsorbed due to the presence of 50 ppm PSS. Thus PSS is able to reduce the amount of AAS binding to silica surfaces under the investigated conditions. Also in the mixed experiment shows that flushing finally with Milli-Q water shows a complete desorption. With a lower PSS concentration of 20 ppm, a similar reduced AAS adsorption had been observed in Fig. S7. The core flooding experiments also revealed the potential of PSS to inhibit surfactant adsorption and an economic analysis of PSS indicates that addition of PSS in surfactant flooding is still be cost-effective when the surfactant price is as low as $1/lb [29].

In the co-injection of AAS and PSS experiments, the competitive adsorption mechanism of an AAS + PSS mixture at water-silica interface is proposed in Fig. 7b. Due to multiple anionic charged sites of PSS, it adsorbed more easily on silica surfaces, which corresponded to the difficult removal in the desorption process. After PSS adsorption, a higher surface coverage with PSS inhibited the adsorption of AAS surfactant because of electrostatic repulsions. It means that PSS and AAS compete for adsorption sites, but the adsorption of PSS was more favored. We can find a considerably lower amount of adsorption of AAS surfactant in the mixture adsorption experiments. It seems more beneficial if the surfactant flooding was first flushed with a polyelectrolyte flooding, rather than simply using simultaneous injection of polyelectrolytes and surfactants.

4. Conclusion

The anionic surfactant AAS adsorbs to silica surfaces readily by the presence of calcium ions. These calcium ions serve as bridges between the negatively charged silica surface and the anionic surfactant head group. For enhanced oil recovery, surfactant binding means the loss of a valuable component. Owning to that reason it is of importance to know how to reduce the amount of AAS binding. For the first time, QCM-D provides real-time quantitative analysis of the surfactant adsorption process in the presence of calcium ion and polystyrene sulfonate on

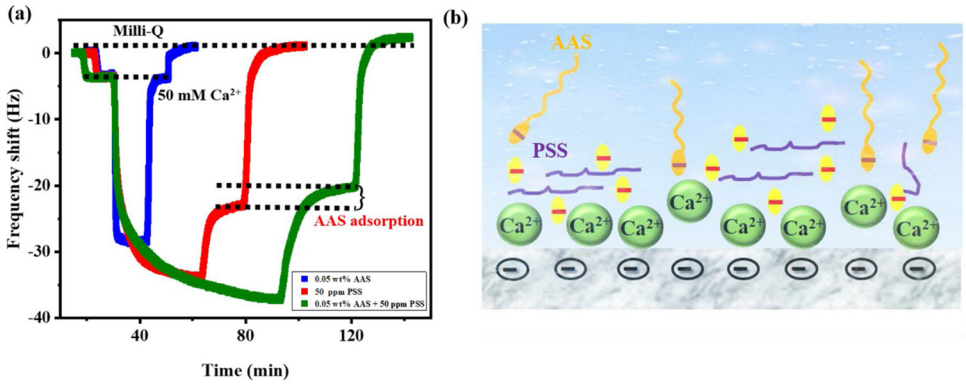

Fig. 7. (a) Real-time experimental data of frequency shifts for dynamic adsorption of AAS, PSS, and an AAS + PSS mixture onto silica surfaces. The contribution of AAS adsorption to the total adsorption in the mixture is evaluated by the difference between desorption of PSS and desorption of the AAS + PSS mixture. (b) Schematic diagram of the competitive adsorption mechanism of the AAS + PSS mixture at the water-silica interface.

silica surfaces, allowing relatively fast and sensitive for screening important experimental parameters. The adsorption of AAS surfactant was found to increase with increasing surfactant concentration until a critical concentration, which was well described by the Langmuir adsorption isotherm. We have performed most of our experiments at pH = 9.5 resembling conditions often applied in EOR. At that pH, the silica surface is highly negatively charged given a high site density for AAS binding via calcium ion bridging. Indeed we found that decreasing the pH (less alkaline) of the solution shows a reduction of AAS adsorption, as a direct result of a reduced negative site density on the silica surface. Increasing the $CaCl_2$ concentration in the solution shows an increased AAS adsorption, until a concentration of 50 mM is obtained. At higher $CaCl_2$ concentrations no additional surfactant adsorption was found. Reduction of AAS loss by adsorption to silica surfaces can be obtained by the application of high NaCl concentrations or by the application of minor amounts of PSS. For NaCl it was found that applying a 100 mM solution is able to reduce the AAS adsorption by 50 % in the presence of 50 mM $CaCl_2$. For PSS was found that only 50 ppm PSS was needed to reduce the amount of AAS adsorbed by 85 %, for a situation of 0.05 wt % AAS and 50 mM $CaCl_2$. The obtained detailed information of the AAS adsorption to silica surfaces as function of pH, $CaCl_2$ and NaCl concentrations as well as the presence of polystyrene sulfonate contributes to our understanding and optimization of surfactant injection in enhanced oil recovery processes.

CRediT author statement

Z.L., N.K., and E.J.R.S. supervised the whole work and were involved in funding acquisition and project administration. Z.L. and N.K. conceptualized the study and devised the surfactant adsorption experiments. Z.L. and P.H. did surface characterizations and and surface tensions mesurements. R.H., P.H., A.R.S., and N.K. conducted surfactant and polyelectrolyte adsorption experiments. Z.L., N.K., and E.J.R.S. analyzed the data. Z.L. and E.J.R.S. wrote the paper with input from all authors. All authors contributed to scientific discussions and analysis, and have approved the final version of the manuscript.

Declaration of Competing Interest

The authors declare that they have no known competing financial interests or personal relationships that could have appeared to influence the work reported in this paper.

Acknowledgments

The authors thank Dr. M. Brewer and Dr. J. van Wunnik (Shell Global Solutions) for providing surfactant samples and for their active discussions. Financial support was provided by Shell Global Solutions.

Appendix A. Supplementary data

Supplementary material related to this article can be found, in the online version, at doi:https://doi.org/10.1016/j.colsurfa.2020.125074.

References

[1] M.S. Kamal, I.A. Hussein, A.S. Sultan, Review on surfactant flooding: phase behavior, retention, IFT, and field applications, Energy Fuels 31 (8) (2017) 7701–7720.
[2] C. Chen, J. Lu, W. Jing, M. Zhou, M. Zhu, W. Xing, Novel external-loop CO2-lift reactor for desilication of alkaline/surfactant/polymer produced water from oil well, Chem. Eng. J. 332 (2018) 66–75.
[3] X. Li, Q. Xue, L. Zhu, Y. Jin, T. Wu, Q. Guo, H. Zheng, S. Lu, How to select an optimal surfactant molecule to speed up the oil-detachment from solid surface: a computational simulation, Chem. Eng. Sci. 147 (2016) 47–53.
[4] G. Hirasaki, C.A. Miller, M. Puerto, Recent advances in surfactant EOR, SPE J. 16 (4) (2011) 889–907.
[5] L.W. Lake, R.T. Johns, W.R. Rossen, G.A. Pope, Fundamentals of Enhanced Oil Recovery, (2014).
[6] M. Tagavifar, S.H. Jang, H. Sharma, D. Wang, L.Y. Chang, K. Mohanty, G.A. Pope, Effect of PH on adsorption of anionic surfactants on limestone: experimental study and surface complexation modeling, Colloids Surf. Physicochem. Eng. Asp. 538 (2018) 549–558.
[7] S.D. Elias, A.M. Rabiu, O. Oluwaseun, B. Seima, Adsorption Characteristics of Surfactants on Different Petroleum Reservoir Materials, (2016).
[8] M.A. Ahmadi, S.R. Shadizadeh, Experimental investigation of a natural surfactant adsorption on shale-sandstone reservoir rocks: static and dynamic conditions, Fuel 159 (2015) 15–26.
[9] A. Durán-Álvarez, M. Maldonado-Domínguez, O. González-Antonio, C. Durán-Valencia, M. Romero-Ávila, F. Barragán-Aroche, S. López-Ramírez, Experimental–theoretical approach to the adsorption mechanisms for anionic, cationic, and zwitterionic surfactants at the calcite–Water interface, Langmuir 32 (11) (2016) 2608–2616.
[10] Z. Liu, M.K. Ghatkesar, E.J. Sudholter, B. Singh, N. Kumar, Understanding the cation dependent surfactant adsorption on clay minerals in oil recovery, Energy Fuels 33 (12) (2019) 12319–12329.
[11] P. Somasundaran, L. Zhang, Adsorption of surfactants on minerals for wettability control in improved oil recovery processes, J. Pet. Sci. Eng. 52 (1–4) (2006) 198–212.
[12] A. Barati, A. Najafi, A. Daryasafar, P. Nadali, H. Moslehi, Adsorption of a new nonionic surfactant on carbonate minerals in enhanced oil recovery: experimental and modeling study, Chem. Eng. Res. Des. 105 (2016) 55–63.
[13] R. Zhang, P. Somasundaran, Advances in adsorption of surfactants and their mixtures at Solid/Solution interfaces, Adv. Colloid Interface Sci. 123 (2006) 213–229.
[14] S. Park, E.S. Lee, W.R.W. Sulaiman, Adsorption behaviors of surfactants for chemical flooding in enhanced oil recovery, J. Ind. Eng. Chem. 21 (2015) 1239–1245.
[15] Al, D. Mahrouqi, J. Vinogradov, M.D. Jackson, Zeta potential of artificial and natural calcite in aqueous solution, Adv. Colloid Interface Sci. 240 (2017) 60–76.
[16] N. Saxena, A. Kumar, A. Mandal, Adsorption analysis of natural anionic surfactant for enhanced oil recovery: the role of mineralogy, salinity, alkalinity and nanoparticles, J. Pet. Sci. Eng. 173 (2019) 1264–1283.
[17] K. Hu, A.J. Bard, Characterization of adsorption of sodium dodecyl sulfate on charge-regulated substrates by atomic force microscopy force measurements, Langmuir 13 (20) (1997) 5418–5425.
[18] J.J. Hamon, A. Striolo, R.F. Tabor, B.P. Grady, AFM force mapping analysis of an adsorbed surfactant above and below the CMC, Langmuir 34 (25) (2018) 7223–7239.
[19] A. Al-Khafaji, A. Neville, M. Wilson, D. Wen, Effect of low salinity on the oil desorption efficiency from calcite and silica surfaces, Energy Fuels 31 (11) (2017) 11892–11901.
[20] S. Solairaj, C. Britton, D.H. Kim, U. Weerasooriya, G.A. Pope, Measurement and analysis of surfactant retention, SPE Improved Oil Recovery Symposium; Society of Petroleum Engineers (2012).

[21] K. Ma, L. Cui, Y. Dong, T. Wang, C. Da, G.J. Hirasaki, S.L. Biswal, Adsorption of cationic and anionic surfactants on natural and synthetic carbonate materials, J. Colloid Interface Sci. 408 (2013) 164–172.
[22] A. Bera, T. Kumar, K. Ojha, A. Mandal, Adsorption of surfactants on sand surface in enhanced oil recovery: isotherms, kinetics and thermodynamic studies, Appl. Surf. Sci. 284 (2013) 87–99.
[23] T. Austad, A. RezaeiDoust, T. Puntervold, Chemical mechanism of low salinity water flooding in sandstone reservoirs, SPE Improved Oil Recovery Symposium; Society of Petroleum Engineers (2010).
[24] M. Lashkarbolooki, S. Ayatollahi, M. Riazi, Mechanistical study of effect of ions in smart water injection into carbonate oil reservoir, Process Saf. Environ. Prot. 105 (2017) 361–372.
[25] R.M. Haaring, N. Kumar, D. Bosma, L. Poltorak, E.J. Sudholter, Electrochemically-assisted deposition of calcite for application in surfactant adsorption studies, Energy Fuels 33 (2) (2019) 805–813.
[26] Z. Salari, M.A. Ahmadi, Experimental studies of ionic surfactant adsorption onto carbonate rocks, Energy Sources Part Recovery Util. Environ. Eff. 38 (4) (2016) 549–554.
[27] E.J. Wanless, W.A. Ducker, Weak influence of divalent ions on anionic surfactant surface-aggregation, Langmuir 13 (6) (1997) 1463–1474.
[28] H. ShamsiJazeyi, R. Verduzco, G.J. Hirasaki, Reducing adsorption of anionic surfactant for enhanced oil recovery: part II. Applied aspects, Colloids Surf. Physicochem. Eng. Asp. 453 (2014) 168–175.
[29] M. Budhathoki, S.H.R. Barnee, B.-J. Shiau, J.H. Harwell, Improved oil recovery by reducing surfactant adsorption with polyelectrolyte in high saline brine, Colloids Surf. Physicochem. Eng. Asp. 498 (2016) 66–73.
[30] H. ShamsiJazeyi, R. Verduzco, G.J. Hirasaki, Reducing adsorption of anionic surfactant for enhanced oil recovery: part I. Competitive adsorption mechanism, Colloids Surf. Physicochem. Eng. Asp. 453 (2014) 162–167.
[31] W.L. Ng, D. Rana, G.H. Neale, V. Hornof, Physicochemical behavior of mixed surfactant systems: petroleum sulfonate and lignosulfonate, J. Appl. Polym. Sci. 88 (4) (2003) 860–865.
[32] J.S. Weston, J.H. Harwell, B.J. Shiau, M. Kabir, Disrupting admicelle formation and preventing surfactant adsorption on metal oxide surfaces using sacrificial polyelectrolytes, Langmuir 30 (22) (2014) 6384–6388.
[33] A. Lager, K.J. Webb, C.J.J. Black, Impact of brine chemistry on oil recovery, IOR 2007-14th European Symposium on Improved Oil Recovery (2007).
[34] S. Adkins, P.J. Liyanage, P. Arachchilage, W.P. Gayani, T. Mudiyanselage, U. Weerasooriya, G.A. Pope, A new process for manufacturing and stabilizing high-performance EOR surfactants at low cost for high-temperature, high-salinity oil reservoirs, SPE Improved Oil Recovery Symposium; Society of Petroleum Engineers (2010).
[35] G. Sauerbrey, Verwendung von Schwingquarzen Zur Wägung Dünner Schichten Und Zur Mikrowägung, Z. Für Phys. 155 (2) (1959) 206–222.
[36] M. Nourani, T. Tichelkamp, B. Gaweł, G. Øye, Method for determining the amount of crude oil desorbed from silica and aluminosilica surfaces upon exposure to combined low-salinity water and surfactant solutions, Energy Fuels 28 (3) (2014) 1884–1889.
[37] K.K. Kanazawa, J.G. Gordon, Frequency of a quartz microbalance in contact with liquid, Anal. Chem. 57 (8) (1985) 1770–1771.
[38] M.M. Ayad, A.A. El-Nasr, Adsorption of cationic dye (methylene blue) from water using polyaniline nanotubes base, J. Phys. Chem. C 114 (34) (2010) 14377–14383.
[39] K.Y. Foo, B.H. Hameed, Insights into the modeling of adsorption isotherm systems, Chem. Eng. J. 156 (1) (2010) 2–10.
[40] B. Samiey, M. Dargahi, Kinetics and thermodynamics of adsorption of Congo red on cellulose, Open Chem. 8 (4) (2010) 906–912.
[41] M.R. Azam, I.M. Tan, L. Ismail, M. Mushtaq, M. Nadeem, M. Sagir, Static adsorption of anionic surfactant onto crushed Berea sandstone, J. Pet. Explor. Prod. Technol. 3 (3) (2013) 195–201.
[42] Z.L. Liu, T. Rios-Carvajal, M.P. Andersson, M. Ceccato, S.L.S. Stipp, T. Hassenkam, Insights into the pore-scale mechanism for the low-salinity effect: implications for enhanced oil recovery, Energy Fuels 32 (12) (2018) 12081–12090.
[43] L. Wang, I. Siretanu, M.H. Duits, M.A.C. Stuart, F. Mugele, Ion effects in the adsorption of carboxylate on oxide surfaces, studied with quartz crystal microbalance, Colloids Surf. Physicochem. Eng. Asp. 494 (2016) 30–38.
[44] J.J. Hamon, R.F. Tabor, A. Striolo, B.P. Grady, Atomic force microscopy force mapping analysis of an adsorbed surfactant above and below the critical micelle concentration, Langmuir 34 (25) (2018) 7223–7239.
[45] T. Wangchareansak, V.S. Craig, S.M. Notley, Adsorption isotherms and structure of cationic surfactants adsorbed on mineral oxide surfaces prepared by atomic layer deposition, Langmuir 29 (48) (2013) 14748–14755.
[46] Z. Liu, T. Rios-Carvajal, M.P. Andersson, S. Stipp, T. Hassenkam, Ion effects on molecular interaction between graphene oxide and organic molecules, Environ. Sci. Nano 6 (7) (2019) 2281–2291.
[47] E.M. Moujahid, J. Inacio, J.-P. Besse, F. Leroux, Adsorption of styrene sulfonate vs. polystyrene sulfonate on layered double hydroxides, Microporous Mesoporous Mater. 57 (1) (2003) 37–46.